

Uranium(VI) Bis(imido) Chalcogenate Complexes: Synthesis and Density Functional Theory Analysis

Liam P. Spencer,[†] Ping Yang,[‡] Brian L. Scott,[†] Enrique R. Batista,[‡] and James M. Boncella^{*†}*Materials, Physics and Applications Division, Los Alamos National Laboratory, MS J514, Los Alamos, New Mexico 87545, and Theoretical Division, Los Alamos National Laboratory, MS B268, Los Alamos, New Mexico 87545*

Received November 18, 2008

Bis(imido) uranium(VI) *trans*- and *cis*-dichalcogenate complexes with the general formula $U(N^iBu)_2(EAr)_2(OPPh_3)_2$ ($EAr = O-2\text{-}^iBuC_6H_4$, SPh, SePh, TePh) and $U(N^iBu)_2(EAr)_2(R_2bpy)$ ($EAr = SPh, SePh, TePh$) ($R_2bpy = 4,4'$ -disubstituted-2,2'-bipyridyl, $R = Me, ^iBu$) have been prepared. This family of complexes includes the first reported monodentate selenolate and telluroate complexes of uranium(VI). Density functional theory calculations show that covalent interactions in the U–E bond increase in the *trans*-dichalcogenate series $U(N^iBu)_2(EAr)_2(OPPh_3)_2$ as the size of the chalcogenate donor increases and that both 5f and 6d orbital participation is important in the M–E bonds of U–S, U–Se, and U–Te complexes.

Introduction

The significance of covalent interactions and the role of f-orbitals in metal ligand bonds in f-element complexes is an intensely studied and greatly debated area in actinide chemistry. Studies of uranyl (UO_2^{2+}) complexes have been crucial in developing an understanding of the importance of these issues in f-element complexes, in particular their function in the formation of U=O multiple bonds.¹ The interactions of ligands in the equatorial plane perpendicular to the dioxo ligands are also important because of the relevance of the UO_2^{2+} ion in lanthanide/actinide separation schemes and speciation of the UO_2^{2+} ion in the environment. Coordination chemistry studies of this ion have shown that the majority of complexes involve hard donor ligands (i.e., O, N, and halide)² which suggests that the equatorial U–L bonds possess significant ionic character.³ The coordination of soft donor ligands to the UO_2^{2+} ion holds promise for

further understanding covalency and f-orbital participation in U–L bonding; however, few of these complexes have been reported.⁴

We have recently reported the isolation of the imido analogue of the uranyl ion ($U(NR)_2^{2+}$) and found that there are some striking differences between this ion and the uranyl ion.⁵ Density functional theory (DFT) calculations and X-ray absorption near edge structure (XANES) experiments have shown that there is less positive charge present on the uranium center in the $U(NR)_2^{2+}$ ion, which suggests a greater degree of covalency in the U=N bond in comparison to the U=O bond in the UO_2^{2+} ion.^{5a} We have also found that soft phosphine donor ligands can coordinate to the $U(NR)_2^{2+}$ ion in contrast to the UO_2^{2+} fragment.^{5b,d} This finding suggests that the metal center in the $U(NR)_2^{2+}$ ion is a softer Lewis acid than its UO_2^{2+} counterpart which presents the op-

* To whom correspondence should be addressed. E-mail: boncella@lanl.gov.

[†] Materials, Physics and Applications Division.

[‡] Theoretical Division.

- (1) (a) Grenthe, I. et. al. In *The Chemistry of the Actinide and Transactinide Elements*, 3rd ed.; Morss, L. R., Edelstein, N. M., Fuger, J., Eds.; Springer-Verlag: New York, 2006; Vol. 1, pp 253–698.
- (2) (a) Bagnall, K. W. I. In *Comprehensive Coordination Chemistry*; Pergamon: Oxford, 1987; Vol. 3, p 1187. (b) King, R. B. *J. Coord. Chem.* **2005**, 58, 47. (c) Szabo, Z.; Toraiishi, T.; Vallet, V.; Grenthe, I. *Coord. Chem. Rev.* **2006**, 250, 784.
- (3) Pierloot, K.; van Besien, E. *J. Chem. Phys.* **2005**, 123, 204309.

- (4) (a) Kannan, S.; Barnes, C. L.; Duval, P. B. *Inorg. Chem.* **2005**, 44, 9137. (b) Crawford, M. J.; Ellern, A.; Noth, H.; Suter, M. *J. Am. Chem. Soc.* **2003**, 125, 11778. (c) Berthet, J. C.; Nierlich, M.; Ephritikhine, M. *Chem. Commun.* **2004**, 870. (d) Crawford, M. J.; Ellern, A.; Karaghiosoff, K.; Mayer, P.; Noth, H.; Suter, M. *Inorg. Chem.* **2004**, 43, 7120. (e) Rose, D.; Chang, Y. D.; Chen, Q.; Zubieta, J. *Inorg. Chem.* **1994**, 33, 5167. (f) Rose, D. J.; Chen, Q.; Zubieta, J. *Inorg. Chim. Acta* **1998**, 268, 163. (g) Crawford, M. J.; Mayer, P. *Inorg. Chem.* **2005**, 44, 5547.
- (5) (a) Hayton, T. W.; Boncella, J. M.; Scott, B. L.; Palmer, P. D.; Batista, E. R.; Hay, P. *J. Science* **2005**, 310, 1941. (b) Hayton, T. W.; Boncella, J. M.; Scott, B. L.; Batista, E. R. *J. Am. Chem. Soc.* **2006**, 128, 10549. (c) Spencer, L. P.; Yang, P.; Scott, B. L.; Batista, E. R.; Boncella, J. M. *J. Am. Chem. Soc.* **2008**, 130, 2930. (d) Spencer, L. P.; Gdula, R. L.; Hayton, T. W.; Scott, B. L.; Batista, E. R.; Boncella, J. M. *Chem. Commun.* **2008**, 4986.

portunity to investigate the coordination of other soft donor ligands and evaluate how covalent interactions and orbital participation in U(VI)–L bonds change as the softness of the L donor is varied.

In this paper, we report the synthesis of a family of bis(imido) uranium(VI) dichalcogenate complexes $U(N^iBu)_2(EAr)_2(OPPh_3)_2$ ($EAr = O-2\text{-}^iBuC_6H_4$, SPh, SePh, TePh) and $U(N^iBu)_2(EAr)_2(R_2bpy)$ ($EAr = SPh, SePh, TePh$) ($R_2bpy = 4,4'$ -disubstituted-2,2'-bipyridyl, $R = Me, ^iBu$). DFT calculations have been performed on the *trans*-dichalcogenate complexes $U(N^iBu)_2(EAr)_2(OPPh_3)_2$ to investigate the trends in covalent interactions as the size of the chalcogenate donor changes and to evaluate the participation of d- and f-orbitals in the U–E bonds.

Experimental Section

Methods and Materials. All reactions and subsequent manipulations were performed under anaerobic and anhydrous conditions under either a high vacuum or an atmosphere of helium or argon. Hexanes and tetrahydrofuran (THF) were dried by passage over activated alumina, and CH_2Cl_2 was purchased anhydrous and stored over activated 4 Å molecular sieves for 24 h before use. CD_2Cl_2 and C_5D_5N were dried over activated 4 Å molecular sieves for 24 h before use. $U(N^iBu)_2I_2(OPPh_3)_2$,^{5b} NaSPh-1/4 dme (dme = $CH_3OCH_2CH_2OCH_3$),⁶ $KO(2\text{-}^iBuC_6H_4)$ ⁷ were synthesized by published procedures or derivations based on published procedures. All other reagents were purchased from commercial suppliers and used as received. NMR spectra were recorded on a Bruker AVA300 spectrometer. 1H and $^{13}C(^1H)$ NMR spectra are referenced to external $SiMe_4$ using the residual protio solvent peaks as internal standards (1H NMR experiments) or the characteristic resonances of the solvent nuclei (^{13}C NMR experiments). The $^{31}P(^1H)$ NMR spectra were referenced to external 85% H_3PO_4 . The $^{77}Se(^1H)$ NMR spectrum was referenced to external Ph_2Se_2 which has a chemical shift of 460 ppm relative to Me_2Se . The $^{125}Te(^1H)$ NMR spectrum was referenced to external Ph_2Te_2 which has a chemical shift of 420 ppm relative to Me_2Te . Elemental analyses were performed at the UC Berkeley Microanalytical Facility on a Perkin-Elmer Series II 2400 CHNS analyzer.

Synthesis of NaEPh-S ($E = Se, S = 1/2$ DME; $E = Te, S = 1/2$ THF). The following procedure is representative of the synthesis of NaEPh-S. To a stirring DME (3 mL) suspension of Na metal (31.3 mg, 1.4 mmol) at room temperature was added a DME solution (2 mL) of Ph_2Se_2 (250 mg, 0.8 mmol). The pale yellow suspension was stirred overnight at which time a yellow solution had formed. The solution was filtered through Celite, and the solvent removed until a white precipitate began to form. Hexanes were added, and the solution was left at $-30\text{ }^\circ C$ overnight to complete precipitation of a powdery white solid (95% yield based on Na metal used). The solid was filtered, dried in vacuo, and identified by 1H NMR spectroscopy. In the case of NaTePh, the residue was recrystallized from THF/hexanes and recovered as a white powder. **NaSePh-1/2 DME:** 1H NMR (C_5D_5N): 3.28 (s, 3H, $-OCH_3$), 3.50 (s, 2H, $-OCH_2$), 6.94–6.97 (m, 3H, $-p\text{-}ArH$ and $-m\text{-}ArH$), 8.32 (d, $^3J(H,H) = 4$ Hz, 2H, $-o\text{-}ArH$). **NaTePh-1/2 THF:** 1H NMR (C_5D_5N): 1.62 (m, 2H, THF), 3.66 (m, 2H, THF), 6.86

(m, 2H, $-m\text{-}ArH$), 7.05 (m, 1H, $-p\text{-}ArH$), 8.65 (d, $^3J(H,H) = 6$ Hz, 2H, $-o\text{-}ArH$).

Synthesis of $U(N^iBu)_2(EAr)_2(OPPh_3)_2$ ($EAr = O-2\text{-}^iBuC_6H_4$ (1), SPh (2), SePh (3), TePh (4)). The following procedure is representative of the synthesis of 1–4. To a cooled ($-30\text{ }^\circ C$) THF (5 mL) solution of $U(N^iBu)_2I_2(OPPh_3)_2$ (175 mg, 0.15 mmol) in a 20 mL scintillation vial was added a chilled ($-30\text{ }^\circ C$) THF solution (2 mL) of $KO-2\text{-}^iBuC_6H_4$ (55.4 mg, 0.30 mmol). The mixture slowly darkens upon warming to room temperature. After being stirred overnight, the brown suspension was filtered through Celite, and the solvent removed until several milliliters remained. Hexanes (10 mL) were added to precipitate a dark red-brown powder (138 mg, 76%), which was recrystallized from CH_2Cl_2 /hexanes. **1:** (Yield = 76%) 1H NMR (C_6D_6): δ 0.33 (s, 18H, $-NC(CH_3)_3$), 2.15 (s, 18H, $-C(CH_3)_3$), 6.89–7.08 (m, 22H, $-OPPh_3$ and $-ArH$), 7.85 (d, $^3J(H,H) = 9$ Hz, 2H, $-ArH$), 8.03 (d, 2H, $^3J(H,H) = 9$ Hz, $-ArH$), 8.25–8.29 (m, 12H, $-OPPh_3$). $^{13}C(^1H)$ NMR (C_6D_6): δ 18.6 ($-C(CH_3)_3$), 35.9 ($-NC(CH_3)_3$), 40.9 ($C(CH_3)_3$), 67.0 ($-NC(CH_3)_3$), 123.7 ($-ArC$), 128.6 ($-ArC$), 129.9 ($-ArC$), 130.5 ($-ArC$), 133.4 ($-ArC$), 135.6 ($-ArC$), 137.8 ($^1J(C,P) = 14$ Hz, $-ArC$), 146.8 ($-ArC$). $^{31}P(^1H)$ NMR (C_6D_6): δ 42.7. **Anal. Calcd. for $C_{64}H_{74}UN_2O_4P_2$:** %C, 62.23; %H, 5.94; %N, 2.27. Found: %C, 62.09; %H, 5.56; %N, 2.16. **2:** (Yield = 86%) 1H NMR (C_6D_6): δ 0.25 (s, 18H, $-NC(CH_3)_3$), 6.88 (t, $^3J(H,H) = 8$ Hz, 4H, $-m\text{-}ArH$), 7.11–7.24 (m, 20H, $-OPPh_3$ and $-p\text{-}ArH$), 8.31 (d, 4H, $^3J(H,H) = 8$ Hz, $-o\text{-}ArH$), 8.53–8.62 (m, 12H, $-ArH$, $-OPPh_3$). $^{13}C(^1H)$ NMR (C_6D_6): δ 35.4 ($-C(CH_3)_3$), 65.3 ($-C(CH_3)_3$), 124.8 ($-ArC$), 128.2 ($-ArC$), 129.2 ($-ArC$), 131.4 ($-ArC$), 134.1 ($-ArC$), 134.8 ($-ArC$), 136.8 ($^1J(C,P) = 14$ Hz, $-ArC$), 143.5 ($-ArC$). $^{31}P(^1H)$ NMR (C_6D_6): δ 43.6. **Anal. Calcd. for $C_{56}H_{58}UN_2O_2P_2S_2$:** %C, 58.22; %H, 5.06; %N, 2.43. Found: %C, 58.74; %H, 4.54; %N, 2.30. **3:** (Yield = 81%) 1H NMR (CD_2Cl_2): δ -0.17 (s, 18H, $-NC(CH_3)_3$), 6.91 (t, $^3J(H,H) = 8$ Hz, 4H, $-m\text{-}ArH$), 7.04 (t, $^3J(H,H) = 8$ Hz, 2H, $-p\text{-}ArH$), 7.42–7.72 (m, 18H, $-OPPh_3$), 8.12 (d, 4H, $^3J(H,H) = 8$ Hz, $-o\text{-}ArH$), 8.41–8.56 (m, 12H, $-OPPh_3$). $^{13}C(^1H)$ NMR (CD_2Cl_2): δ 36.8 ($-C(CH_3)_3$), 66.1 ($-C(CH_3)_3$), 122.9 ($-ArC$), 127.6 ($-ArC$), 128.6 ($-ArC$), 130.2 ($-ArC$), 133.3 ($-ArC$), 135.8 ($-ArC$), 137.0 ($^1J(C,P) = 14$ Hz, $-ArC$), 145.2 ($-ArC$). $^{31}P(^1H)$ NMR (CD_2Cl_2): δ 43.7. $^{77}Se(^1H)$ NMR (CD_2Cl_2): δ 134.3. **Anal. Calcd. for $C_{56}H_{58}UN_2O_2P_2Se_2$:** %C, 53.85; %H, 4.68; %N, 2.24. Found: %C, 53.32; %H, 4.55; %N, 2.39. **4:** (Yield = 73%) 1H NMR (CD_2Cl_2): δ -0.11 (s, 18H, $-NC(CH_3)_3$), 6.94 (t, $^3J(H,H) = 8$ Hz, 4H, $-m\text{-}ArH$), 7.52–7.68 (m, 18H, $-OPPh_3$), 7.18 (t, $^3J(H,H) = 8$ Hz, $-p\text{-}ArH$), 8.06 (d, 4H, $^3J(H,H) = 8$ Hz, $-o\text{-}ArH$), 8.37–8.51 (m, 12H, $-ArH$, $-OPPh_3$). $^{13}C(^1H)$ NMR (CD_2Cl_2): δ 34.9 ($-C(CH_3)_3$), 64.9 ($-C(CH_3)_3$), 121.6 ($-ArC$), 127.1 ($-ArC$), 127.9 ($-ArC$), 129.8 ($-ArC$), 134.7 ($-ArC$), 135.1 ($-ArC$), 136.3 ($^1J(C,P) = 14$ Hz, $-ArC$), 142.5 ($-ArC$). $^{31}P(^1H)$ NMR (CD_2Cl_2): δ 44.3. $^{125}Te(^1H)$ NMR (CD_2Cl_2): δ 216.8. **Anal. Calcd. for $C_{56}H_{58}UN_2O_2P_2Te_2$:** %C, 49.96; %H, 4.34; %N, 2.08. Found: %C, 49.78; %H, 4.07; %N, 2.38.

Synthesis of $U(N^iBu)_2(I_2)(R_2bpy)$ ($R = Me$ (5), iBu (6)). The following procedure is representative of the synthesis of 5 and 6. A toluene (5 mL) solution of $U(N^iBu)_2(I_2)(THF)_2$ (500 mg, 0.64 mmol) was treated with a toluene (2 mL) solution of Me_2bpy (118 mg, 0.64 mmol) and stirred for 2 h. The red-orange precipitate was collected by filtration and washed with toluene (2×5 mL) and dried in vacuo. (526 mg, Yield = 97%), **5:** 1H NMR (CD_2Cl_2): δ 0.12 (s, 18H, $-C(CH_3)_3$), 2.77 (s, 6H, $-CH_3$), 7.90 (d, $^3J(H,H) = 5$ Hz, 2H, $-bpyH$), 8.60 (s, 2H, $-bpyH$), 10.74 (d, $^3J(H,H) = 5$ Hz, 2H, $-bpyH$). $^{13}C(^1H)$ NMR (CD_2Cl_2): δ 29.3 ($-C(CH_3)_3$), 34.2 ($-CH_3$), 72.3 ($-C(CH_3)_3$), 122.6 ($-bpyC$), 124.6 ($-bpyC$), 148.2 ($-bpyC$), 155.7 ($-bpyC$), 165.0 ($-bpyC$). **Anal. Calcd. For**

(6) Bartucz, T. Y.; Golombek, A.; Lough, A. J.; Maltby, P. A.; Morris, R. H.; Ramachandran, R.; Schlaf, M. *Inorg. Chem.* **1998**, *37*, 1555.

(7) Buzzeo, M. C.; Zakharov, L. N.; Rheingold, A. L.; Doerrer, L. H. *J. Mol. Struct.* **2003**, *657*, 19.

C₂₀H₃₀N₄I₂U: %C 29.36; %H, 3.70; %N, 6.85. Found: %C, 29.44; %H, 3.62; %N, 6.66. **6**: ¹H NMR (CD₂Cl₂): δ 0.12 (s, 18H, -C(CH₃)₃), 1.59 (s, 6H, -C(CH₃)₃), 8.08 (d, ³J(H,H) = 5 Hz, 2H, -bpyH), 8.66 (s, 2H, -bpyH), 10.80 (d, ³J(H,H) = 5 Hz, 2H, -bpyH). ¹³C(¹H) NMR (CD₂Cl₂): δ 30.5 (-C(CH₃)₃), 30.7 (-C(CH₃)₃), 55.4 (-C(CH₃)₃), 76.5 (-C(CH₃)₃), 121.2 (-bpyC), 123.5 (-bpyC), 149.1 (-bpyC), 157.2 (-bpyC), 166.0 (-bpyC). **Anal. Calcd. For C₂₆H₄₂N₄I₂U**: %C, 34.60; %H, 4.69; %N, 6.21. Found: %C, 34.52; %H, 4.52; %N, 6.15.

Synthesis of U(NⁱBu)₂(EPH)₂(R₂bpy) (E = S, R = Me (7); E = S, R = ⁱBu (8); E = Se, R = Me (9); E = Se, R = ⁱBu (10); E = Te, R = Me (11); E = Te, R = ⁱBu (12)). The following procedure is representative of the synthesis of 7–12. To a cooled (-30 °C) THF (5 mL) solution of **5** (175 mg, 0.21 mmol) in a 20 mL scintillation vial was added a chilled (-30 °C) THF solution (2 mL) of NaSPh-1/4 dme (95 mg, 0.42 mmol). The mixture slowly turns a deep red color upon warming to room temperature. After being stirred overnight, the red suspension was filtered through Celite, and the solvent removed until several milliliters remained. Hexanes (10 mL) were added to precipitate a bright red powder (138 mg, 76%), which was recrystallized from CH₂Cl₂/hexanes. (mg, Yield = %) **7**: ¹H NMR (CD₂Cl₂): δ -0.29 (s, 18H, -C(CH₃)₃), 2.74 (s, 6H, -CH₃), 6.86 (t, *J* = 7 Hz, 2H, -*p*-SArH), 7.21 (t, ³J(H,H) = 7 Hz, 4H, -*m*-SArH), 7.89 (d, ³J(H,H) = 5 Hz, 2H, -*H*), 8.09 (d, ³J(H,H) = 7 Hz, 4H, -*o*-SArH), 8.50 (s, 2H, -bpyH), 10.85 (d, ³J(H,H) = 5 Hz, 2H, -bpyH). ¹³C(¹H) NMR (CD₂Cl₂): δ 29.9 (-C(CH₃)₃), 35.0 (-CH₃), 71.3 (-C(CH₃)₃), 122.9 (-bpyC), 123.8 (-ArC), 125.9 (-bpyC), 128.6 (-ArC), 147.1 (-bpyC), 152.2 (-ArC), 153.5 (-bpyC), 164.2 (-bpyC). **Anal. Calcd. For C₃₂H₄₀N₄S₂U**: %C, 49.09; %H, 5.15; %N, 7.19. Found: %C, 48.98; %H, 5.07; %N, 7.11. **8**: Three molecules of THF were present in the solid state lattice. Under vacuum, the crystalline material obtained readily loses this solvent. ¹H NMR (CD₂Cl₂): δ -0.29 (s, 18H, -C(CH₃)₃), 1.58 (s, 18H, -C(CH₃)₃), 6.87 (t, *J* = 7 Hz, 2H, -*p*-SArH), 7.22 (t, ³J(H,H) = 7 Hz, 4H, -*m*-SArH), 8.10 (br s, 6H, -bpyH and -*o*-SArH), 8.60 (s, 2H, -bpyH), 10.89 (d, ³J(H,H) = 5 Hz, 2H, -bpyH). ¹³C(¹H) NMR (CD₂Cl₂): δ 32.3 (-C(CH₃)₃), 33.0 (-C(CH₃)₃), 53.2 (-C(CH₃)₃), 75.8 (-C(CH₃)₃), 123.4 (-bpyC), 125.3 (-ArC), 125.9 (-bpyC), 129.1 (-ArC), 133.7 (-ArC), 149.0 (-bpyC), 150.6 (-ArC), 152.9 (-bpyC), 163.3 (-bpyC). **Anal. Calcd. For C₃₈H₅₂N₄S₂U**: %C, 52.64; %H, 6.05; %N, 6.46. Found: %C, 52.59; %H, 6.13; %N, 6.37. **9**: ¹H NMR (CD₂Cl₂): δ -0.21 (s, 18H, -C(CH₃)₃), 2.75 (s, 6H, -CH₃), 6.95 (t, *J* = 7 Hz, 2H, -*p*-SeArH), 7.19 (t, ³J(H,H) = 7 Hz, 4H, -*m*-SArH), 7.90 (d, ³J(H,H) = 5 Hz, 2H, -bpyH), 8.23 (d, ³J(H,H) = 7 Hz, 4H, -*o*-SArH), 8.53 (s, 2H, -bpyH), 10.87 (d, ³J(H,H) = 5 Hz, 2H, -bpyH). ¹³C(¹H) NMR (CD₂Cl₂): δ 29.3 (-C(CH₃)₃), 35.7 (-CH₃), 72.5 (-C(CH₃)₃), 123.6 (-bpyC), 124.8 (-ArC), 127.4 (-bpyC), 129.1 (-ArC), 148.0 (-bpyC), 151.6 (-ArC), 153.0 (-bpyC), 165.3 (-bpyC). ⁷⁷Se(¹H) NMR (CD₂Cl₂): δ 142.8. **Anal. Calcd. For C₃₂H₄₀N₄Se₂U**: %C, 43.84; %H, 4.71; %N, 6.39. Found: %C, 43.80; %H, 4.71; %N, 6.29. **10**: ¹H NMR (CD₂Cl₂): δ -0.23 (s, 18H, -C(CH₃)₃), 1.58 (s, 18H, -C(CH₃)₃), 6.95 (t, ³J(H,H) = 8 Hz, 2H, -*p*-SeArH), 7.18 (t, ³J(H,H) = 7 Hz, 4H, -*m*-SeArH), 8.08 (d, ³J(H,H) = 5 Hz, 2H, -bpyH), 8.26 (d, ³J(H,H) = 7 Hz, 4H, -*o*-SeArH), 8.60 (s, 2H, -bpyH), 10.90 (d, ³J(H,H) = 5 Hz, 2H, -bpyH). ¹³C(¹H) NMR (CD₂Cl₂): δ 30.2 (-C(CH₃)₃), 30.6 (-C(CH₃)₃), 55.5 (-C(CH₃)₃), 77.2 (-C(CH₃)₃), 124.9 (-bpyC), 125.6 (-ArC), 125.3 (-bpyC), 129.9 (-ArC), 134.1 (-ArC), 149.5 (-bpyC), 150.0 (-ArC), 153.1 (-bpyC), 165.8 (-bpyC). ⁷⁷Se(¹H) NMR (CD₂Cl₂): δ 145.0. **Anal. Calcd. For C₃₈H₅₂N₄Se₂U**: %C, 47.50; %H, 5.46; %N, 5.83. Found: %C, 47.61; %H, 5.60; %N, 5.72. **11**: ¹H NMR (CD₂Cl₂): δ -0.10 (s, 18H, -C(CH₃)₃), 1.89 (s, 18H, -C(CH₃)₃), 6.79 (t, ³J(H,H) = 8 Hz, 2H,

-*p*-TeArH), 7.01 (t, ³J(H,H) = 7 Hz, 4H, -*m*-TeArH), 7.50 (³J(H,H) = 5 Hz, 2H, -bpyH), 8.19 (d, ³J(H,H) = 7 Hz, 4H, -*o*-TeArH), 8.97 (s, 2H, -bpyH), 11.06 (d, ³J(H,H) = 5 Hz, 2H, -bpyH). ¹³C(¹H) NMR (CD₂Cl₂): δ 30.5 (-C(CH₃)₃), 34.2 (-CH₃), 73.9 (-C(CH₃)₃), 121.7 (-bpyC), 124.0 (-ArC), 126.3 (-bpyC), 129.4 (-ArC), 146.2 (-bpyC), 153.1 (-ArC), 155.0 (-bpyC), 163.9 (-bpyC). ¹²⁵Te(¹H) NMR (CD₂Cl₂): δ 226.3. **Anal. Calcd. For C₃₂H₄₀N₄Te₂U**: %C, 39.46; %H, 4.14; %N, 5.75. Found: %C, 39.40; %H, 4.21; %N, 5.71. **12**: ¹H NMR (CD₂Cl₂): δ -0.092 (s, 18H, -C(CH₃)₃), 1.56 (s, 18H, -C(CH₃)₃), 6.91 (t, ³J(H,H) = 8 Hz, 2H, -*p*-TeArH), 7.07 (t, ³J(H,H) = 7 Hz, 4H, -*m*-TeArH), 7.51 (d, ³J(H,H) = 5 Hz, 2H, -bpyH), 8.24 (d, ³J(H,H) = 7 Hz, 4H, -*o*-TeArH), 8.83 (s, 2H, -bpyH), 10.93 (d, ³J(H,H) = 5 Hz, 2H, -bpyH). ¹³C(¹H) NMR (CD₂Cl₂): δ 31.0 (-C(CH₃)₃), 31.2 (-C(CH₃)₃), 53.6 (-C(CH₃)₃), 75.3 (-C(CH₃)₃), 123.8 (-bpyC), 124.2 (-ArC), 124.9 (-bpyC), 128.6 (-ArC), 133.0 (-ArC), 148.6 (-bpyC), 151.4 (-ArC), 152.6 (-bpyC), 164.6 (-bpyC). ¹²⁵Te(¹H) NMR (CD₂Cl₂): δ 224.0. **Anal. Calcd. For C₃₈H₅₂N₄Te₂U**: %C, 43.13; %H, 4.95; %N, 5.30. Found: %C, 42.98; %H, 4.88; %N, 5.23.

X-ray Crystallographic Details. The crystal structures of compounds **1–4**, **5**, **8**, **9**, and **12** were determined as follows: The crystal was mounted in a nylon cryoloop from Paratone-N oil under argon gas flow. The data were collected on a Bruker SMART APEX II charge-coupled-device (CCD) diffractometer, with KRYO-FLEX liquid nitrogen vapor cooling device. The instrument was equipped with graphite monochromatized Mo K α X-ray source ($\lambda = 0.71073$ Å), with MonoCap X-ray source optics. A hemisphere of data was collected using ω scans, with 5 s frame exposures and 0.3° frame widths. Data collection and initial indexing and cell refinement were handled using APEX II software.⁸ Frame integration, including Lorentz-polarization corrections, and final cell parameter calculations were carried out using the SAINT+ software.⁹ The data were corrected for absorption using the SADABS program.¹⁰ Decay of reflection intensity was monitored via analysis of redundant frames. The structure was solved using Direct methods and difference Fourier techniques. All hydrogen atom positions were idealized, and rode on the atom they were attached to. The final refinement included anisotropic temperature factors on all non-hydrogen atoms. Structure solution, refinement, graphics, and creation of publication materials were performed using SHELXTL.¹¹

Computational Details. The B3LYP hybrid density functional was employed to optimize the equilibrium molecular structures of all the complexes studied.¹² The small-core Stuttgart RSC 1997 relativistic effective core potential (RECP) was used to model the uranium center,¹³ with the associate basis set [6s/6p/5d/3f]. For light chalcogenate atoms, that is, oxygen, sulfur, and selenium, the 6-31+G* basis sets were used. While for the heavy chalcogenate atoms, selenium, tellurium, and polonium, the calculations use the Stuttgart relativistic large core ECP.¹⁴ To compare systematically and avoid spurious effects while comparing all-electron calculations with pseudopotential ones, we also applied the same Stuttgart ECP on oxygen and sulfur complexes. The geometries of all the molecules were optimized without symmetry constraints. The geometries from the all electron and RECP calculation were

(8) APEX II, 1.08; Bruker AXS, Inc.: Madison, WI, 2004; S15.

(9) SAINT+, 7.06; Bruker AXS, Inc.: Madison, WI, 2003.

(10) Sheldrick, G. M. SADABS, 2.03; University of Göttingen: Göttingen, Germany, 2001.

(11) SHELXTL, 5.10; Bruker AXS, Inc.: Madison, WI, 1997.

(12) Becke, A. D. *J. Chem. Phys.* **1993**, *98*, 5648.

(13) Küchle, W.; Dolg, M.; Stoll, H.; Preuss, H. *J. Chem. Phys.* **1994**, *100*, 7535.

(14) (a) Fuentealba, P.; Preuss, H.; Stoll, H.; Szentpaly, L. v. *Chem. Phys. Lett.* **1982**, *89*, 418–422. (b) Kuechle, W.; Dolg, M.; Stoll, H.; Preuss, H. *Mol. Phys.* **1991**, *74*, 1245–1263.

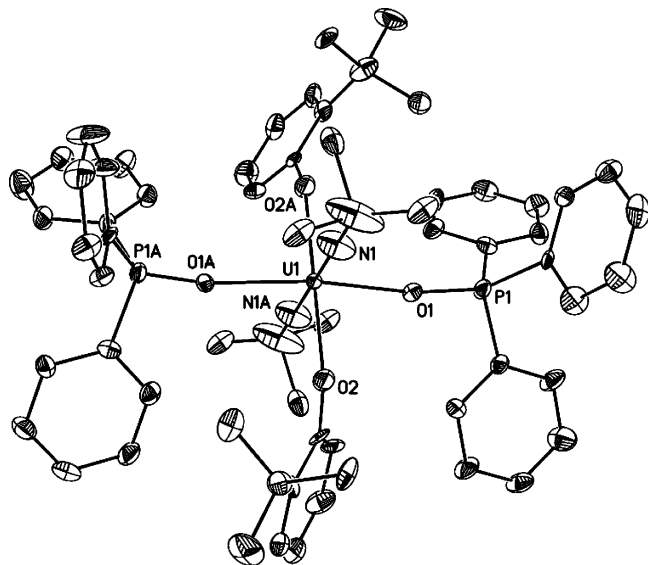


Figure 1. Solid state molecular structure of $[U(N^tBu)_2(O-2-tBuC_6H_4)_2(OPPh_3)_2]$ (**1**) with thermal ellipsoids drawn at the 50% probability level (Symmetry codes: (A) $-x, 1 - y, z$). Selected bond lengths (Å) and angles (deg): U1–N1 = 1.870(6), U1–O1 = 2.341(7), U1–O2 = 2.267(6), O1–P1 = 1.539(7), N1–U1–N1A = 180.0, U1–O2–C5 = 145.1(4).

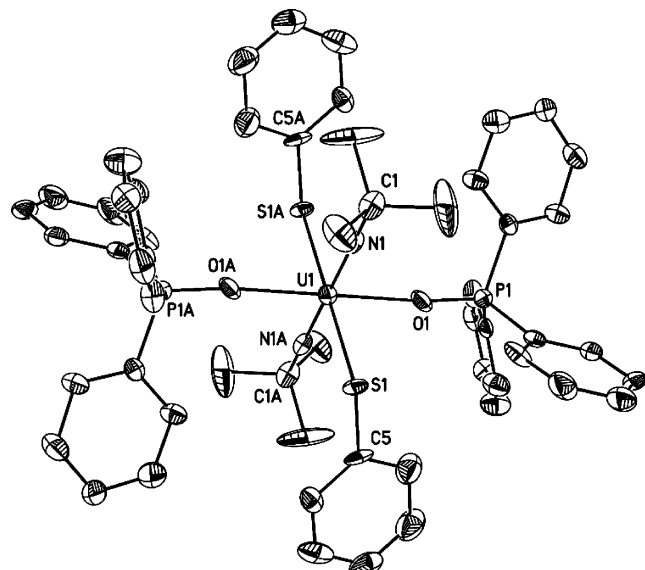


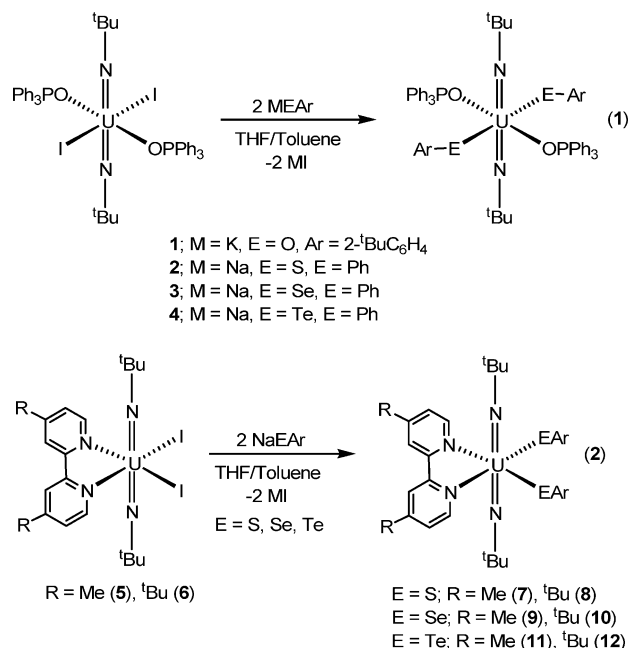
Figure 2. Solid state molecular structure of $[U(N^tBu)_2(SPh)_2(OPPh_3)_2]$ (**2**) with thermal ellipsoids drawn at the 50% probability level. Selected bond lengths (Å) and angles (deg): U1–N1 = 1.840(7), U1–S1 = 2.757(10), U1–O1 = 2.322(5), O1–P1 = 1.533(6), U1–S1–C5 = 110.6(2), N1–U1–N1A = 180.0.

essentially identical and in good agreement with the experimental structures (see below). The molecular orbital energies from the two methodologies are equivalent and the components of the orbitals are the same. All the calculations reported in this paper were carried out with the Gaussian 03 code.¹⁵

Results and Discussion

We have previously shown that the iodide ligands in the bis(imido) uranium(VI) complex $U(NR)_2(I)_2(THF)_x$ ($R = tBu, x = 2; Ph, x = 3$) can undergo metathesis reactions to generate new uranium(VI) complexes.^{5b} Rather than use these uranium(VI) synthons as an entry to chalcogenate complexes, we focused on the reactivity of the triph-

enylphosphine oxide analogue, $U(N^tBu)_2(I)_2(OPPh_3)_2$, which has enabled us to follow reactions by ³¹P NMR spectroscopy. The reactions between 2 equiv of aryl chalcogenate reagents MEAr ($M = K, EAr = O-2-tBuC_6H_4$; $M = Na, EAr = SPh, SePh, TePh$) and $U(N^tBu)_2(I)_2(OPPh_3)_2$ provide the uranium(VI) *trans*-dichalcogenate complexes $U(N^tBu)_2(EAr)_2(OPPh_3)_2$ (**1–4**, eq 1). The *cis*-dichalcogenate complexes $U(N^tBu)_2(EAr)_2(R_2bpy)$ ($EAr = SPh, SePh, TePh$) (**7–12**, eq 2) were prepared in a similar fashion from the bis(imido) uranium(VI) diiodide complexes $U(N^tBu)_2(I)_2(R_2bpy)$ (**5, 6**). To our knowledge, the selenolate and tellurolate complexes in this family of complexes represent the first monodentate uranium(VI)-selenolate and -tellurolate complexes reported. The ¹H NMR spectrum of **1** is representative and features two equivalent ^tBu-phenoxide donors with a singlet at 2.15 ppm and multiplets at 7.85, 8.03, and 8.27 ppm. In addition, there are multiplets at 6.90 and 8.27 ppm indicative of the OPPh₃ ligands and a singlet at 0.33 ppm attributable to the *tert*-butyl imido group. The ³¹P NMR of **1** shows a singlet at 42.7 ppm that is shifted downfield from the starting material $U(N^tBu)_2(I)_2(OPPh_3)_2$. An interesting aspect of compounds **3** and **4** is the ⁷⁷Se(¹H) and ¹²⁵Te(¹H)NMR spectra that feature singlets at 134.3 and 216.8 ppm, respectively. Similar ⁷⁷Se and ¹²⁵Te chemical shifts were also observed in the *cis*-dichalcogenate complexes **9–12**.



Reactions between the *cis*-disposed diiodide complexes **5** and **6** and 2 equiv of NaOR ($R = C_6H_5, 4-MeC_6H_4, 2-tBuC_6H_4$) give unexpected products. Instead of the anticipated bis(imido) uranium(VI) bis(phenolate) complexes, a family of mixed valent uranium(V)–uranium(VI) complexes was recovered that have been identified by NMR spectroscopy and X-ray diffraction experiments. A full description of these complexes will be published in due course.

We have also explored the reactions between 2 equiv of NaEPh ($E = Se, Te$) and $UO_2I_2(OPPh_3)_2$ in an attempt to form analogous selenolate and tellurolate complexes of the UO_2^{2+}

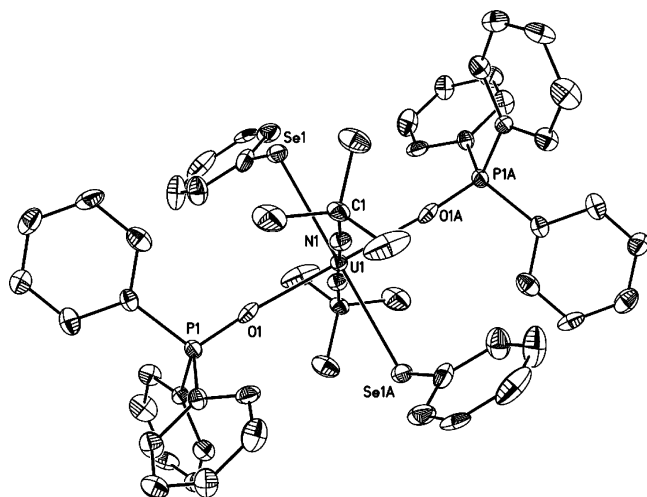


Figure 3. Solid state molecular structure of $[U(N^tBu)_2(SePh)_2(OPPh_3)_2]$ (**3**) with thermal ellipsoids drawn at the 50% probability level. Selected bond lengths (Å) and angles (deg): U1–N1 = 1.861(6), U1–Se1 = 2.8868(8), U1–O1 = 2.360(5), O1–P1 = 1.483(6), N1–U1–N1A = 180.0, U1–Se1–C5 = 106.4(2).

ion. Given the simple nature of these compounds and the extensive coordination studies performed with the uranyl ion, it is surprising that these complexes have yet to be reported. Our attempts to prepare these complexes did not provide unidentifiable materials as evidenced by 1H NMR spectroscopy. Similar findings were observed in a previous study that examined the coordination of unidentate thiolate ligands to the UO_2^{2+} ion. In this report, stable mononuclear uranylthiolate complexes were only isolated with monodentate thiolate ligands that possessed significant electron-withdrawing properties and provided steric protection at the uranium(VI) center.^{4a} In light of these findings and our failed attempts to prepare simple Se- and Te-analogues of the UO_2^{2+} ion, it appears that the nature of the uranium center in the $U(NR)_2^{2+}$ and UO_2^{2+} ions has a significant effect on the isolation of stable uranium(VI) chalcogenate complexes. This striking difference has facilitated the isolation of novel uranium(VI) complexes with unique U(VI)–E bonds (E = S, Se, Te, P).

The solid state molecular structures of **1–5**, **8**, **9**, and **12** were determined by X-ray crystallography. Their respective thermal ellipsoid plots are shown in Figures 1–7. In the case of **4**, there is considerable disorder among the phos-

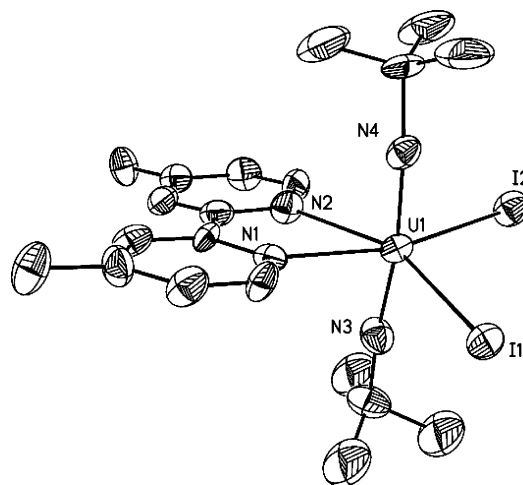


Figure 4. Solid state molecular structure of $[U(N^tBu)_2(I)_2(Me_2bpy)]$ (**5**) with thermal ellipsoids drawn at the 50% probability level. Selected bond lengths (Å) and angles (deg): U1–N1 = 2.530(11), U1–N2 = 2.480(10), U1–N3 = 1.822(11), U1–N4 = 1.810(11), U1–I1 = 3.0526(15), U1–I2 = 3.0115(18), N1–U1–N2 = 64.2(3), N3–U1–N4 = 171.3(5), I1–U1–I2 = 105.11(4).

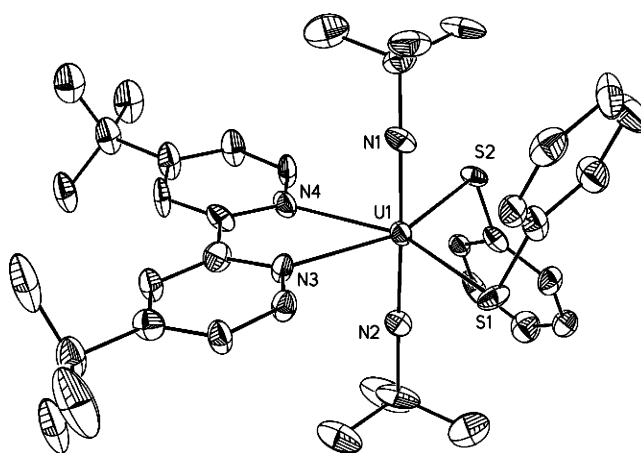


Figure 5. Solid state molecular structure of $[U(N^tBu)_2(SPh)_2(Bu_2bpy)]$ (**8**) with thermal ellipsoids drawn at the 50% probability level. Selected bond lengths (Å) and angles (deg): U1–N1 = 1.835(11), U1–N2 = 1.846(11), U1–N3 = 2.565(11), U1–N4 = 2.533(12), U1–S1 = 2.690(3), U1–S2 = 2.682(3), N1–U1–N2 = 178.4(5), N3–U1–N4 = 62.2(4), U1–S1–C27 = 108.0(5), U1–S2–C33 = 110.1(4).

phine oxide and imido ligands. Despite this disorder, the structure confirms the substitution at the uranium center (see Supporting Information, Figure 1S) and possesses a small estimated standard deviation for U–Te bond distances and angles. Selected average bond lengths and angles of both *trans*- and *cis*-dichalcogenate complexes are shown in Table 1. Complexes with the general formula $U(N^tBu)_2(EAr)_2(OPPh_3)_2$ (**1–4**) are isostructural and feature a uranium center in a *pseudo*-octahedral geometry with imido, aryl chalcogenate, and phosphine oxide ligands in an all *trans*-disposition. The U–N(imido), U–I, and U–O(phosphine oxide) bond lengths are all comparable to analogous bond lengths in other structurally characterized uranium bis(imido) complexes.⁵ The U1–O2 phenolate bond length in **1** is 2.267(6) Å and is longer than the U–O phenolate bond distances in the

(15) Frisch, M. J.; Trucks, G. W.; Schlegel, H. B.; Scuseria, G. E.; Robb, M. A.; Cheeseman, J. R.; Montgomery, J. J. A.; Vreven, T.; Kudin, K. N.; Burant, J. C.; Millam, J. M.; Iyengar, S. S.; Tomasi, J.; Barone, V.; Mennucci, B.; Cossi, M.; Scalmani, G.; Rega, N.; Petersson, G. A.; Nakatsuji, H.; Hada, M.; Ehara, M.; Toyota, K.; Fukuda, R.; Hasegawa, J.; Ishida, M.; Nakajima, T.; Honda, Y.; Kitao, O.; Nakai, H.; Klene, M.; Li, X.; Knox, J. E.; Hratchian, H. P.; Cross, J. B.; Bakken, V.; Adamo, C.; Jaramillo, J.; Gomperts, R.; Stratmann, R. E.; Yazyev, O.; Austin, A. J.; Cammi, R.; Pomelli, C.; Ochterski, J. W.; Ayala, P. Y.; Morokuma, K.; Voth, G. A.; Salvador, P.; Dannenberg, J. J.; Zakrzewski, V. G.; Dapprich, S.; Daniels, A. D.; Strain, M. C.; Farkas, O.; Malick, D. K.; Rabuck, A. D.; Raghavachari, K.; Foresman, J. B.; Ortiz, J. V.; Cui, Q.; Baboul, A. G.; Clifford, S.; Cioslowski, J.; Stefanov, B. B.; Liu, G.; Liashenko, A.; Piskorz, P.; Komaromi, I.; Martin, R. L.; Fox, D. J.; Keith, T.; Al-Laham, M. A.; Peng, C. Y.; Nanayakkara, A.; Challacombe, M.; Gill, P. M. W.; Johnson, B.; Chen, W.; Wong, M. W.; Gonzalez, C.; Pople, J. A. *Gaussian 03*, Revision C.02; Gaussian, Inc.: Wallingford, CT, 2004.

(16) Wilkerson, M. P.; Burns, C. J.; Morris, D. E.; Paine, R. T.; Scott, B. L. *Inorg. Chem.* **2002**, *41*, 3110.

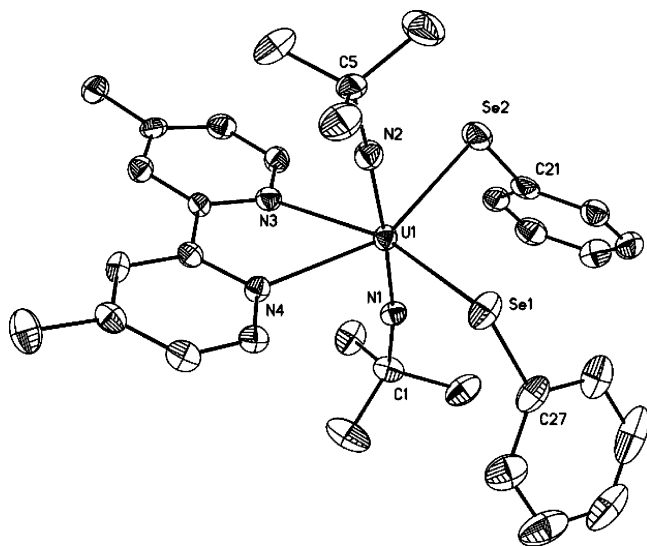


Figure 6. Solid state molecular structure of $[U(N^iBu)_2(SePh)_2(Me_2bpy)]$ (**9**) with thermal ellipsoids drawn at the 50% probability level. Selected bond lengths (\AA) and angles (deg): $U1-N1 = 1.843(4)$, $U1-N2 = 1.846(4)$, $U1-N3 = 2.526(4)$, $U1-N4 = 2.532(4)$, $U1-Se1 = 2.8375(5)$, $U1-Se2 = 2.8073(5)$, $N1-U1-N2 = 175.94(17)$, $N3-U1-N4 = 62.93(12)$, $U1-Se1-C21 = 108.54(14)$, $U1-Se2-C27 = 104.83(14)$.

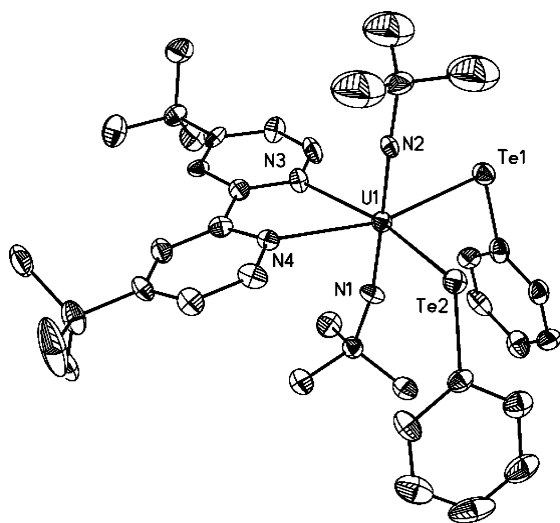


Figure 7. Solid state molecular structure of $[U(N^iBu)_2(TePh)_2(Bu_2bpy)]$ (**12**) with thermal ellipsoids drawn at the 50% probability level. Selected bond lengths (\AA) and angles (deg): $U1-N1 = 1.824(8)$, $U1-N2 = 1.832(8)$, $U1-N3 = 2.544(8)$, $U1-N4 = 2.521(8)$, $U1-Te1 = 3.0405(8)$, $U1-Te2 = 3.0335(8)$, $N1-U1-N2 = 177.4(3)$, $N3-U1-N4 = 63.4(3)$, $U1-Te1-C27 = 100.2(3)$, $U1-Te2-C33 = 103.0(3)$.

neutral monomeric uranium(VI) phenolate complexes $[UO_2(O-2,6-^iBu_2C_6H_3)(THF)_2]$ (avg. $U-O(\text{phenolate}) = 2.200(8) \text{\AA}$),¹⁶ $[UO_2(O-2,6-Ph_2C_6H_3)_2(THF)_2]$ (avg. $U-O(\text{phenolate}) = 2.199(11) \text{\AA}$),¹⁶ and $[UO_2(O-2,6-^iPr_2C_6H_3)_2(py)_3]$ (avg. $U-O(\text{phenolate}) = 2.197(5) \text{\AA}$).¹⁷ The $U(1)-S(1)$ bond distance of $2.757(10) \text{\AA}$ in **2** is slightly longer than the bond lengths reported for the unidentate thiolate uranium(VI) complex $[UO_2(S-2,6-Cl_2C_6H_3)L_2]$ (avg. = $2.7234(8) \text{\AA}$)^{4a} but shorter than the bond lengths reported for $[UO_2(o-C_5H_4NS)(NO_3)_2]^-$ ($2.805(6) \text{\AA}$) and $[UO_2(o-C_5H_4NS-3-SiMe_3)(NO_3)_2]$ ($2.813(8) \text{\AA}$).^{4f} The $U(1)-Se(1)$ bond length

of $2.8868(8) \text{\AA}$ in **3** is significantly shorter than the only other structurally characterized uranium(VI) compound that has a $U-Se$ bond, $[UO_2[Et_2NCSe_2]_2(Ph_3AsO)]$ (average $U-Se$ bond length = $2.981(5) \text{\AA}$)¹⁸ but is longer than the terminal $U-Se$ bond distances found in the uranium-(IV) selenolate complex $[U(SePh)_2(\mu-SePh)_2(CH_3CN)_2]$ ($U-Se_{\text{terminal}} = 2.8491(12) \text{\AA}$).¹⁹ In the case of complex **4**, the $U(1)-Te(1)$ bond lengths ($3.0920(13) \text{\AA}$) possess a small estimated standard deviation and are shorter than the average $U-Te$ bond reported lengths in the uranium (III) species $U(N(Te^iPr)_2)_3$ ($U-Te = 3.1639(7) \text{\AA}$)²⁰ but longer than average $U-Te$ bond lengths in the uranium(IV) complex $(C_5Me_5)_2U(TePh)_2$ ($U-Te = 3.0444(6) \text{\AA}$).²¹ *cis*-Disposed dichalcogenate complexes **5**, **8**, **9**, and **12** possess structural features that are similar to their *trans*-oriented congeners. The diiodo complex **5** possesses $U-N(\text{imido})$ and $U-I$ bond lengths typical of many bis(imido) uranium(VI) complexes. The $U-N(\text{bpy})$ bond lengths are also similar to bipyridyl complexes of the uranyl(VI) ion.²² The $U-E$ chalcogenate bond lengths in **8**, **9**, and **12** have values are similar to those in the *trans*-series.

These structural studies reveal a trend in the $U-E-C_{\text{ipso}}$ angles of the *trans*-series **1–4** and the *cis*-series **8**, **9**, and **12**. In **1**, a $U(1)-O(2)-C(5)$ bond angle of $145.1(4)^\circ$ is observed that gradually decreases in going to the heavier chalcogenate donor complexes **2** ($U(1)-S(1)-C(5) = 110.0(6)^\circ$), **3** ($U(1)-Se(1)-C(5) = 106.4(2)^\circ$), and **4** ($U(1)-Te(1)-C(5) = 103.9(3)^\circ$). The family of *cis*-dichalcogenate complexes shows a similar decrease from the thiolate complex **8** ($109.1(5)^\circ$) to the heavier selenolate complex **9** ($106.69(14)^\circ$) and telluroate complex **12** ($101.6(3)^\circ$). This trend of a decreasing $U-E-C_{\text{ipso}}$ bond angle has also been observed in $(C_5Me_5)_2U(EPh)_2$ ($E = S, Se, Te$)²¹ and $(C_5Me_5)_2Sm(EPh)THF$ ($E = S, Se, Te$)²³ complexes and is consistent with a decrease in the degree of s hybridization of the E atoms in the $U-E$ bond as the atomic number of E increases.

Theoretical Calculations

The series of $U(N^iBu)_2(EAr)_2(OPPh_3)_2$ compounds was studied using hybrid density functional theory (DFT) to investigate trends in the covalency and the participation of f -orbitals in the $U-E$ bonds. The polonium analogue, $U(N^iBu)_2(PoPh)_2(OPPh_3)_2$ (**5**), was also studied to complete the chalcogenate series. The optimized structures of $U(N^iBu)_2(EAr)_2(OPPh_3)_2$ as predicted by DFT calculations are shown in Table 2 and agree well with $U-E$ bond lengths and $U-E-C_{\text{ipso}}$ bond angles determined from crystal-

(18) Zarli, B.; Graziani, R.; Forselli, E.; Croatto, U.; Bombieri, G. *J. Chem. Soc., Chem. Commun.* **1971**, 1501.

(19) Gaunt, A. J.; Scott, B. L.; Neu, M. P. *Inorg. Chem.* **2006**, *45*, 7401.

(20) Gaunt, A. J.; Scott, B. L.; Neu, M. P. *Angew. Chem., Int. Ed.* **2006**, *45*, 1638.

(21) Evans, W. J.; Miller, K. A.; Ziller, J. W.; Dipasquale, A. G.; Heroux, K. J.; Rheingold, A. L. *Organometallics* **2007**, *26*, 4287.

(22) (a) Alcock, N. W.; Flanders, D. J.; Brown, D. *J. Chem. Soc., Dalton Trans.* **1985**, 1001. (b) Berthet, J. C.; Nierlich, M.; Ephritikhine, M. *Chem. Commun.* **2003**, 1660.

(23) Evans, W. J.; Miller, K. A.; Lee, D. S.; Ziller, J. W. *Inorg. Chem.* **2005**, *44*, 4326.

(17) Barnhart, D. M.; Burns, C. J.; Sauer, N. N.; Watkin, J. G. *Inorg. Chem.* **1995**, *34*, 4079.

Table 1. Selected Average Bond Lengths (Å) and Angles (deg) of *trans*-Dichalcogenates (**1–4**) and *cis*-Dichalcogenates (**8, 9, and 12**)

	1 (E = O)	2 (E = S)	3 (E = Se)	4 (E = Te)	8 (E = S)	9 (E = Se)	12 (E = Te)
U–N _{imido}	1.870(6)	1.840(7)	1.861(6)	1.829(19)	1.841(11)	1.845(4)	1.828(8)
U–E	2.267(6)	2.757(10)	2.8868(8)	3.0920(13)	2.686(3)	2.8224(5)	3.0370(8)
U–O _{ippo}	2.341(7)	2.322(5)	2.360(5)	2.39(2)			
U–N _{bpv}					2.549(12)	2.529(4)	2.532(8)
U–E–C _{ipso}	145.1(4)	110.6(2)	106.4(2)	103.9(3)	109.1(5)	106.69(14)	101.6(3)

Table 2. Comparison of Selected Experimental and Theoretical Metrical Parameters in Complexes **1–5**

E	experimental geometry				at optimized geometry			
	U–E–C _{ipso} (deg)	U–E (Å)	U–OPPh ₃ (Å)	U=N (Å)	U–E–C _{ipso} (deg)	U–E (Å)	U–OPPh ₃ (Å)	U=N (Å)
O	145.06	2.267	2.341	1.870	149.9	2.261	2.451	1.875
S	109.98	2.757	2.322	1.840	119.2	2.791	2.433	1.862
Se	106.43	2.887	2.360	1.861	115.2	2.933	2.431	1.860
Te	103.90	3.092	2.366	1.863	111.8	3.184	2.428	1.857
Po	<i>a</i>	<i>a</i>	<i>a</i>	<i>a</i>	111.1	3.252	2.427	1.856

^a Complex was not synthesized.**Table 3.** Mulliken Charges for the Uranium Center, the N=U=N unit, and the Chalcogenate Atom in U(N^tBu)₂(EAr)₂ (OPPh₃)₂

E	all electron			RECP		
	U	UN ₂	E	U	UN ₂	E
O	1.65	0.41	−0.72	1.64	0.39	−0.71
S	1.36	0.11	−0.21	1.35	0.09	−0.19
Se	1.33	0.07	−0.16	1.34	0.07	−0.15
Te	<i>a</i>	<i>a</i>	<i>a</i>	1.31	0.03	−0.06
Po	<i>a</i>	<i>a</i>	<i>a</i>	1.33	0.04	−0.04

^a Were not calculated.**Table 4.** Molecular Orbitals Involved in the Bonding between the Uranium Center and Chalcogen Donor^a

E	MOs	energy (eV)	U-6d	U-5f	E- <i>np</i> (each)
O	H-2	−5.37	11.3		9.8
	H-8	−6.22		10.1	28.3
	H-9	−6.73	10.1		23.2
S	H-0	−4.54		5.2	26.0
	H-1	−4.75	4.8		27.5
	H-2	−5.12		6.0	42.3
	H-3	−5.41	6.1		35.8
	H-30	−8.30	4.8		9.7
Se	H-0	−4.44		6.1	31.2
	H-1	−4.65	5.4		36.8
	H-2	−4.79		5.9	43.8
	H-3	−5.16	6.9		31.1
	H-11	−6.79	7.5		12.8
	H-26	−7.89	5.8		13.7
Te	H-0	−4.35		6.6	35.9
	H-1	−4.45	5.0		41.9
	H-2	−4.54		5.8	44.1
	H-3	−5.05	8.9		30.5
	H-11	−6.62	10.4		7.8
	H-26	−7.52	8.4		12.9
Po	H-0	−4.19		6.3	38.6
	H-2	−4.34		6.5	43.2
	H-3	−4.94	10.7		31.2
	H-11	−6.54	12.6		5.3
	H-14	−7.02		3.5	12.5
	H-23	−7.32	7.8		11.2

^a Values of the uranium 6d and 5f-orbitals are expressed as the percentage contribution in the specified molecular orbital in the U–E bonds of complexes **1–5**. The participating orbitals are referenced to the highest occupied molecular orbital (HOMO, H-0 means HOMO and H-2 corresponds to HOMO-2 orbital). The values given are the percent contributions from the uranium 6d and 5f orbitals and the *np* orbitals of the chalcogenide atom to each MO.

lographic measurements. In the case of complex **2**, the U–E and U–E–C_{ipso} (E = O, S, Se, Te) values determined by DFT calculations are within 3% and 9° of experimental

findings. Similar discrepancies between experimental and theoretical values have also been observed for other uranium(VI) imido complexes at a similar level of computational theory.²⁴

The amount of electronic charge in (1) the uranium and E centers and (2) the N=U=N core were examined to assess the nature of covalent interactions in the U–E bonds in complexes **1–5**. Table 3 shows a consistent trend where the E center becomes less negative and the U center less positive as the size of the chalcogenate donor increases. For example, a significant decrease in charge in both U and E centers and the N=U=N unit is observed between the O-complex **1** and the S-complex **2**, which suggests that the U–O bond possesses a more ionic character compared to U–S bonds. This finding suggests a monotonic shift in the covalent nature in the U–E bond as the size of the chalcogenate donor increases which is also consistent with previous reports on a series of uranium(III) chalcogenate complexes.²⁵

The relative bonding strength of the U–E bond was evaluated by comparing the interaction energies of the two charged fragments, that is, one [U(N^tBu)₂(OPPh₃)₂]²⁺ unit and two EAr[−] ions, at the geometry of the molecular complex, with the delocalized molecular complexes. The calculations show interaction energies of −160.8, −140.7, −135.7, −129.6, and −127.7 kcal/mol, per EAr[−] unit, for E corresponding to O, S, Se, Te, and Po, respectively. Although these energies are not true values for U–E bond energies because they are in the totally ionic limit, the differences between these numbers show that the relative strength of the U–E bond decreases as the size of chalcogen atom becomes larger.

These results suggest that a correlation exists between covalency and relative U–E bond strength in U(N^tBu)₂(EAr)₂(OPPh₃)₂ complexes. As the size of the E donor is increased, the covalency in the U–E bond increases and the relative U–E bond strength decreases. Recent studies of uranium(IV)–L multiple bonds in Cp₂U=L (L = O, NMe) have also shown this correlation between covalency and U–L bond strength.²⁶ In the case of Cp₂U=O, the U=O bond contains less covalent character compared to the U=N analogue but possesses a stronger U–L multiple bond.

The molecular orbitals involved in the U–E bond are decomposed in uranium 6d and 5f, and chalcogenate *np* component in Table 4. The values are given as percentage of the total MO using a Mulliken population decomposition. For this type of analysis, where one looks at trends in charge migration from one center to another, the Mulliken decomposition gives a reasonable description as the overlap between uranium and chalcogenate basis functions is not large and each center is described by a complete enough basis set. The MOs of complexes **1–5** show significant mixing of uranium 6d and 5f orbitals with the *np* orbitals of the chalcogenate atom (Table 4). This finding suggests covalent interactions are important in the formation of U–E bonds in the family of U(N^tBu)₂(EAr)₂(OPPh₃)₂ complexes.

Conclusion

We have shown that a series of bis(imido) uranium(VI) *trans*- and *cis*-dichalcogenate complexes can be synthesized and report the first examples of monodentate selenolate and telluroate-uranium(VI) complexes. These results further exemplify the differences between UO₂²⁺ and U(NR)₂²⁺ ions, as Se- and Te-donor ligands are not known to coordinate to the UO₂²⁺ ion. DFT calculations show that covalent interactions in the U–E bond increase as the size of the chalcogenate donor increases and that there is both 5f and 6d orbital

participation in the M–E bond of U–S, U–Se, and U–Te complexes. While it is not possible to obtain a quantitative view of covalency in these complexes, it is clear that covalent interactions and f-orbitals are important U(VI)–E bonds in this series of uranium(VI) chalcogenate complexes. We are currently investigating the use X-ray absorption spectroscopy to further evaluate the electronic structure of this family of uranium(VI) complexes.

Acknowledgment. P.Y. and L.S. thank the Seaborg Institute for their postdoctoral fellowships. E.R.B. and J.M.B. were partially supported by the Division of Chemical Sciences, Office of Basic Energy Sciences, U.S. Department of Energy under the Heavy Element Chemistry program at LANL. We thank the Center for Integrated Nanotechnology at LANL for computing support. LANL is operated by Los Alamos National Security, LLC, for the National Nuclear Security Administration of the US DOE under contract DE-AC52-06NA25396.

Supporting Information Available: Complete X-ray crystallographic details (as CIF files) of **1–4**, **5**, **8**, **9**, and **12**. Geometries of the calculated structures of **1–5**. This material is available free of charge via the Internet at <http://pubs.acs.org>.

IC802212M

(24) Graves, C. R.; Yang, P.; Kozimor, S. A.; Vaughn, A. E.; Clark, D. L.; Conradson, S. D.; Schelter, E. J.; Scott, B. L.; Thompson, J. D.; Hay, P. J.; Morris, D. E.; Kiplinger, J. L. *J. Am. Chem. Soc.* **2008**, *130*, 5272.

(25) (a) Gaunt, A. J.; Reilly, S. D.; Enriquez, A. E.; Scott, B. L.; Ibers, J. A.; Sekar, P.; Ingram, K. I. M.; Kaltsoyannis, N.; Neu, M. P. *Inorg. Chem.* **2008**, *47*, 29. (b) Ingram, K. I. M.; Kaltsoyannis, N.; Gaunt, A. J.; Neu, M. P. *J. Alloys Compd.* **2007**, *444–445*, 369.

(26) Barros, N.; Maynau, D.; Maron, L.; Eisenstein, O.; Zi, G. F.; Andersen, R. A. *Organometallics* **2007**, *26*, 5059.